UAV hyperspectral inversion modeling of rice nitrogen content based on WOA-ELM

Fenghua Yu[1,2], Wen Du[1,2], Zhonghui Guo[1], Changxian Zhou[1], Dingkang Wang[1], Tongyu Xu[1,2*]

(1. *College of Information and Electrical Engineering, Shenyang Agricultural University, Shenyang 110866, China*;
2. *Liaoning Agricultural Information Engineering Technology Research Center, Shenyang 110866, China*)

Abstract: Nitrogen content is an important indicator of the growth status of the rice in cold region. It can be obtained in time using UAV hyperspectral remote sensing technology at a regional scale. This study is based on the remote sensing test data of the rice in precision agriculture aviation team experiment station of Shenyang Agricultural University from 2018. The method of Sequent Projection Approach (SPA) was used to extract the effective band including 465 nm, 501 nm, 578 nm, 702 nm and 783 nm. The extracted characteristic band is used as the input, and the inversion models of nitrogen content in rice canopy were established respectively by using the Extreme Learning Machine (ELM), and the Extreme Learning Machine by genetic algorithm (GA-ELM) and by Whale optimization algorithm (WOA-ELM). The results showed that the precision of the nitrogen content of rice based on the WOA-ELM was better than the inversion model established by ELM and GA-ELM. The R^2 of training data is 0.887, the R^2 of test data is 0.880, the RMSE of training data is 0.269, the RMSE of test data is 0.284. This study provides a certain data support and application basis for the diagnosis of rice nitrogen content in cold region by UAV hyperspectral remote sensing technology in northeast China.
Keywords: UAV, nitrogen content, rice in cold region, hyperspectral, WOA-ELM
DOI: 10.33440/j.ijpaa.20190202.39.

1　Introduction

Rice is one of the most important staple crops in China, among which rice grown in northeast China is cold land rice[1]. In cold region, rice has a long growth period, high protein content and good taste[2]. The characteristics of rice in cold area are low temperature in early spring, low temperature and soil temperature after rice transplanting, and Yslow nutrient release, so it is necessary to supplement some chemical fertilizer in key growth period. The nitrogen content of rice can directly reflect the lack of nutrition in the growing process of rice, which is the most important diagnostic index of rice growth[3, 4]. At present, in the process of rice production in the cold region of northeast China, most of the farmers evaluate the lack of nitrogen nutrition in rice by observing the change of leaf color on the spot, and then make the nitrogen topdressing tube based on artificial experience rational decision[5]. UAV low altitude remote sensing platform is a kind of near-earth remote sensing means which has developed rapidly in recent years[6,7]. Compared with other remote sensing means, it has some advantages in flexibility, richness of data acquisition, regional coverage and so on. Therefore, the use of UAV hyperspectral remote sensing method to retrieve and estimate the nitrogen content in the cold rice canopy at the near-earth scale has important practical significance[8] for the field of precision fertilization.

At present, the use of hyperspectral technology to estimate crop nitrogen nutrition diagnosis has made some research results in the world. Yu et al[9]. combined the RTM and GPR to retrieval crop leaf chlorophyll content and effectively monitor nitrogen nutrition of rice. Du et al.[10] established an inversion model of nitrogen content in rice canopy leaves based on the hyperspectral remote sensing technology of UAV and the machine learning algorithm, and the decision coefficient R^2 of the model was 0.8525. Jay et al.[11] exploited the centimeter resolution of UAV multispectral imagery to inversion the nitrogen content in sugar beet crops. Camino et al.[12] improved nitrogen retrievals with airborne-derived fluorescence and plant traits quantified from hyperspectral imagery in the context of precision agriculture. Masemola et al.[13] analyzed the leaf structure interference factors affecting the estimation of leaf nitrogen content, and constructed a characteristic wavelength selection method with R^2 of 0.82 and RMSE of 0.13, besides determined typical nitrogen bands of crop leaves , which can effectively monitor Nitrogen content of leaves during different periods. Klem et al.[13] studied the special and thermal indexes can provide satisfactory estimations of perspective of interactions between water and N discount, grain yield, N uptake, and mathematical responses. However, the water availability should be considered when estimating the grain protein content. At present, in the research of UAV remote sensing inversion of rice, most of them first establish a statistical regression model using the vegetation index, and then invert the chlorophyll content, which have ideal inversion effect for specific varieties in specific areas, but there were still some deficiencies in the universality of the model[14-16]. The previous work of using hyperspectral analysis

technology to detect chlorophyll content mainly focused on two aspects: establishing various vegetation indexes, using multiple linear or non-linear regression method to establish the inversion model between the index and chlorophyll content; or modeling all bands of hyperspectral data of rice canopy by PCA, PLS and other methods[17].   Among them, the vegetation index method had clear physical meaning and simple model construction.   But at present, there are a large number of spectral indexes constructed, which means a single vegetation index cannot well represent the whole hyperspectral   information[18]..   Although   all   hyperspectral information is taken into account in the latter, all bands are needed as model input for each inversion, which requires a large amount of calculation and complicated model application[19].

The purpose of this study was to study the inversion of nitrogen content in the rice canopy and leaf layer in the cold region of Northeast China, so as to solve the problem of rapid, accurate and nondestructive diagnosis of nutrition status in rice growth process and to improve the accuracy of nitrogen content inversion. In order to realize the accurate inversion of rice canopy chlorophyll content in the cold region of northeast China, the study used UAV hyperspectral remote sensing platform to obtain the hyperspectral image data of the key growth period of Japonica rice canopy, and used the successive projection algorithm (SPA) to select the sensitive band of the response of rice nitrogen content, then established the limit learning machine inversion model based on the improved whale optimization algorithm (WOA-ELM).

2   Materials and methods

2.1   Study area and design

This study was carried out in the pilot field of precision agriculture aviation team of Shenyang agricultural university. The pilot place was located in Liutiao Village, Shenyang City, Liaoning Province (123°63′E, 42°01′N), the experiment was carried out from June to August 2018.   The leaf hyperspectral remote sensing data acquisition and rice surface sample collection were carried out in the experimental field.   The experimental variety of rice was "Shennong 9816" and the key growth period of rice in cold regions is divided into three stages: cold stage, jointing stage and heading stage.   In the process of data acquisition, the weather is fine, if it is rainy or not conducive to data acquisition, the acquisition will be postponed.   In order to produce more obvious differences in chlorophyll changes during rice growth, this study designed four cold rice experimental plot nitrogen gradient treatments, namely CK, N1, N2, N3.   Each treatment was repeated three times.   Among them, CK is the control group, i.e. no nitrogen application.N1 is the local standard nitrogen application level, the application amount of nitrogen is 45 kg/hm^2; N2 is the low nitrogen application level, and the application amount is 0.5 times of N1; N3 is the high nitrogen application level, and the application amount is 1.5 times of N1.

As for the application amount of phosphorus and potassium in the four experiment plot is in accordance with the local standard application amount, of which the standard application amount of phosphorus is 51.75 kg/hm^2, and the standard application amount of potassium is 18 kg/hm^2.   The content of total nitrogen in 0-0.5 m arable soil of CK, N1, N2 and N3 test fields was 0.154 mg/kg, 0.162 mg/kg, 0.159 mg/kg and 0.168 mg/kg respectively, and the content of available nitrogen was 104.032 mg/kg, 111.109 mg/kg, 116.771 mg/kg and 127.386 mg/kg respectively.   Other field management shall be carried out according to the local normal level. Figure 1 shows the experimental area of this study.
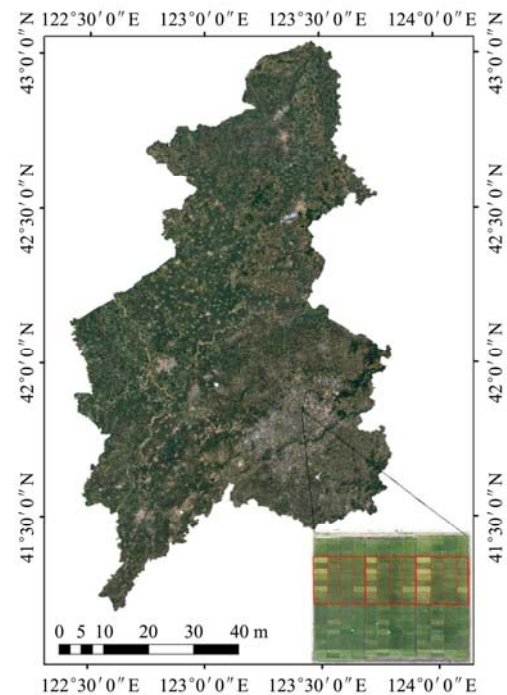

Figure 1   Test site of this study

2.2   UAV hyperspectral image data acquisition

The UAV hyperspectral platform adopts the M600 PRO six-rotor UAV from DJI Co., Ltd. and the hyperspectral imager uses the airborne hyperspectral imaging system from Sichuan Shuangli Hepu Company (Sichuan, China).   The hyperspectral band range is 400-1075 nm, the resolution is 3.5nm, and the number of effective bands is 253.   The hyperspectral imaging system is shown in Figure 2.

Figure 2   UAV Hyperspectral Imaging system

The data acquisition time of hyperspectral remote sensing platform of UAV is between 11:00-12:00 a.m.   in each test, the period with relatively stable solar light intensity is selected, and the flight height of UAV is 100 m.   In this study, the DN value of rice canopy was transformed into the hyperspectral reflectance information of rice canopy by field calibration.   A black and white calibration blanket is placed on the path in the rice field.   The hyperspectral information of the calibration blanket is included in the hyperspectral image collected by the UAV during the hyperspectral acquisition process.   The DN value is converted into the spectral reflectance by formula (1).

$$\rho_t = \frac{DN_t - DN_1}{DN_2 - DN_1}(\rho_2 - \rho_1) + \rho_1 \tag{1}$$

where, ρ_t and DN_t are the reflectance and DN values of the ground object to be converted, and the reflectance of the calibration blanket are ρ_1 and ρ_2, respectively. DN_1 and DN_2 are the DN values of the calibration blanket.

We used the ENVI5.4 software to extract the hyperspectral data of the acquired hyperspectral remote sensing image, firstly using the spectral angle mapping method to remove the influence of interfering object spectra, and then calculating the average spectrum of each area of interest as hyperspectral information for each test plot.

2.3   Measurement of nitrogen content

The key growth period of rice canopy data acquisition in cold region mainly covered three periods of rice Growth: tillering period, jointing period and booting period.   The field sampling work was carried out in the middle growing area of the experimental plot.   Six rice pits were collected in each plot as the sample points of the plot.   30 leaves of the canopy leaves were taken and put into the sealed bag, and then quickly put into the mobile ice chamber for cold preservation.   At the same time, we use the RTK-GPS equipment to collect the geographical coordinates of the sampling points, which is used to correspond with the hyperspectral image data collected by the UAV.

After the rice leaves were brought back to the laboratory, the fresh leaves were placed in the oven and killed out at 105°C for 30min, then dried at 65°C to constant weight.   The traditional Kjeldahl method was used to measure the nitrogen content of the sample after weighing[20].

2.4   Data processing

In this study, a total of 12 experimental data collection were carried out, and the collected data were removed by 3 times standard deviation.   At the same time, combined with the canopy spectral curve, the Monte Carlo algorithm is used to eliminate the abnormal spectral data, and finally 256 samples are obtained.   196 of them are selected as the modeling data set, and the other 60 groups are the validation data set.   The statistical characteristics of the sampling data in this study are shown in Table 1.

Table 1   Statistical characteristics of nitrogen content in rice in experimental plot

Samples	Minimum/%	Maximum/%	Mean/%	SD/%	CV/%
256	7.86	1.11	4.12	25.17	0.48

2.5   Hyperspectral characteristic band selection

In this study, the continuous projection algorithm (SPA) was used to extract hyperspectral information from characteristic spectral bands of the japonica rice canopy, which was then used as the input variable of the chlorophyll content inversion model. SPA is a forward variable selection algorithm that minimizes collinearity in vector space.   The SPA algorithm flow consists of three stages:

In the first stage, a subset of candidate wavelength variables with the smallest collinearity is selected.   Assuming that the initial variable position $k(0)$ and the number of variables N have been given, the specific steps of this stage are as follows.

Step 1: Prior to the first iteration (n=1), assign the j-th column of the training set spectral matrix X_{cal} to X_j, j=1, …, J.

Step 2: Let S be the set of all unselected wavelength variables, i.e.: $S=\{j|1\leq j\leq J$ and $j\notin \{k(0), …, k(n-1)\}\}$.

Step 3: For all $j\notin S$, calculate the projection of X_j on a subspace orthogonal to $X_{k(n-1)}$.

$$\mathrm{P}x_j = x_j - (x_j^T x_{k(n-1)} x_{k(n-1)} (x_j^T x_{k(n-1)} x_{k(n-1)})^{-1} \tag{2}$$

In the formula: P is the projection operator.

$$k(n) = \arg(\max \| \mathrm{P}x_j \|, j\notin S) \tag{3}$$

Step 5: Let $x_j = \mathrm{P}_{xj}, \quad j\notin S$.

Step 6: Let n=n+1.   If $n<N$ then return to step 2 to finish: Obtain N alternative wavelength positions: $\{k(n); n$=0, …, $N-1\}$.

The number of projection operations performed during selection is ($N-1$) ($J-N/2$).

In the second stage, multiple linear regression (MLR) models were established using the variables in each subset to select the subset with the smallest root mean square error (RMSE).

In the third stage, stepwise regression modeling was performed on the subset selected in the second stage, and a set with a smaller number of variables was obtained without the loss of prediction accuracy as much as possible.   The wavelength variable in the set was the selected effective wavelength.

2.6   WOA-ELM inversion modelling of nitrogen content

In this study, the extreme learning machine model based on whale optimization algorithm was used to retrieve the nitrogen content of rice canopy in cold region.   The whale optimization algorithm is used to optimize the input layer weight and hidden layer deviation of the extreme learning machine, so as to calculate the output weight matrix

In this study, the RMSE and coefficient of determination (R^2) were used as evaluation criteria for assessing the accuracy of the UAV hyperspectral remote sensing inversion of inversion of rice canopy nitrogen content in cold area.

3   Results and discussion

3.1   Results of selecting characteristic bands

In this study, SPA was used to extract the characteristic band of nitrogen content in rice canopy in cold region.   Figure 3 is the result of feature band extracted by spa algorithm for hyperspectral information of rice canopy.   The effective wavelengths selected are 465 nm, 501 nm, 578 nm, 702 nm and 783 nm.
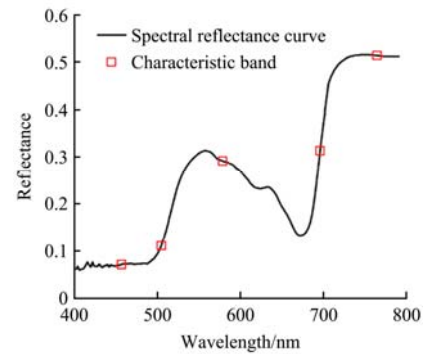

Figure 3   Selection of characteristic bands of SPA in canopy layer of rice

3.2   Inversion results of WOA-ELM for nitrogen content

In this paper, the spectral characteristic band of rice canopy in cold region extracted by SPA is independent variable, and the nitrogen content of rice canopy is dependent variable.   Three methods, ELM, GA-ELM and WOA-ELM, are used to establish the hyperspectral inversion model of rice nitrogen content estimation.   Figure 4 is the demerit of ELM optimized by WOA.

GA and WOA were used to optimize the weight and threshold of elm, and R^2 was selected as the fitness function to evaluate the nitrogen content model.   In order to test the prediction accuracy and learning speed of elm model, the maximum number of iterations of model training is set as 200. R^2 and RMSE performance indexes of model training samples and test samples are selected to compare and analyze the models established by the three methods.   The results of the three modeling methods are shown in Table 2.
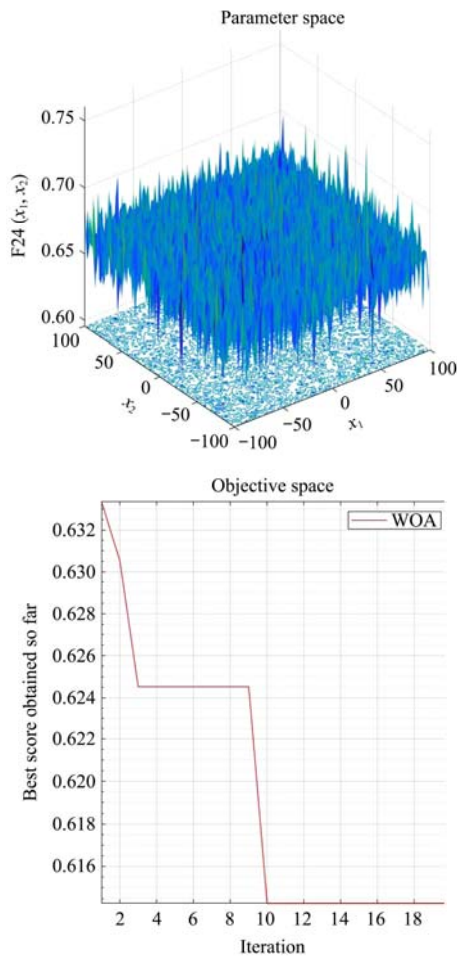
Figure 4   Results of whale optimization algorithm

Table 2   Results of three modeling methods by ELM GA-ELM WOA-ELM

Modeling method	ELM	GA-ELM	WOA-ELM
t/s	7.68	6.11	8.47
R^2	0.808 (train)	0.831 (train)	0.887 (train)
	0.793 (test)	0.828 (test)	0.880 (test)
RMSE	0.326 (train)	0.317 (train)	0.269 (train)
	0.365 (test)	0.344 (test)	0.284 (test)

From the modeling results in Table 2, it can be seen that the above three models can achieve high prediction accuracy in the training samples, but the prediction accuracy of WOA-ELM model is slightly better than the other two models, and its R^2 value is the largest and RMSE value is the smallest in the test samples, which also shows that the model has better generalization ability compared with the other two models.

The inversion effect of the traditional limit learning machine algorithm is slightly lower than that of the inversion model established by the genetic optimization algorithm and the whale optimization algorithm. This is mainly because the weight and threshold of the traditional ELM are given automatically when modeling, not the optimal solution. GA and WOA are used to optimize the weight and threshold setting of elm model, which can effectively obtain the optimal solution, so better inversion accuracy can be obtained.

3.3   Precision analysis of nitrogen content inversion model

Although the accuracy of the model is better than that of the traditional ELM and GA-ELM, the performance of the model in various engineering fields is still to be studied due to the relatively late time of WOA. WOA simulates the predatory behavior of whales in the ocean and optimizes the search by surrounding whales and attacking prey with bubbles. It is consistent with the classical particle swarm algorithm, ant colony algorithm and artificial bee colony algorithm, which is essentially a process of statistical optimization. Because of the advantages of simple operation, few parameters and excellent performance, WOA algorithm has been widely concerned by many scholars and applied to different practical problems. However, WOA algorithm is easy to fall into the local optimum, and the algorithm stagnates in the later stage. The inversion accuracy of nitrogen content established by the three methods is shown in Figure 5. In the model adopted in this study, WOA-ELM has the highest accuracy, the R^2 of training data is 0.887, the R^2 of test data is 0.880, the RMSE of training data is 0.269, the RMSE of test data is 0.284.

a. ELM

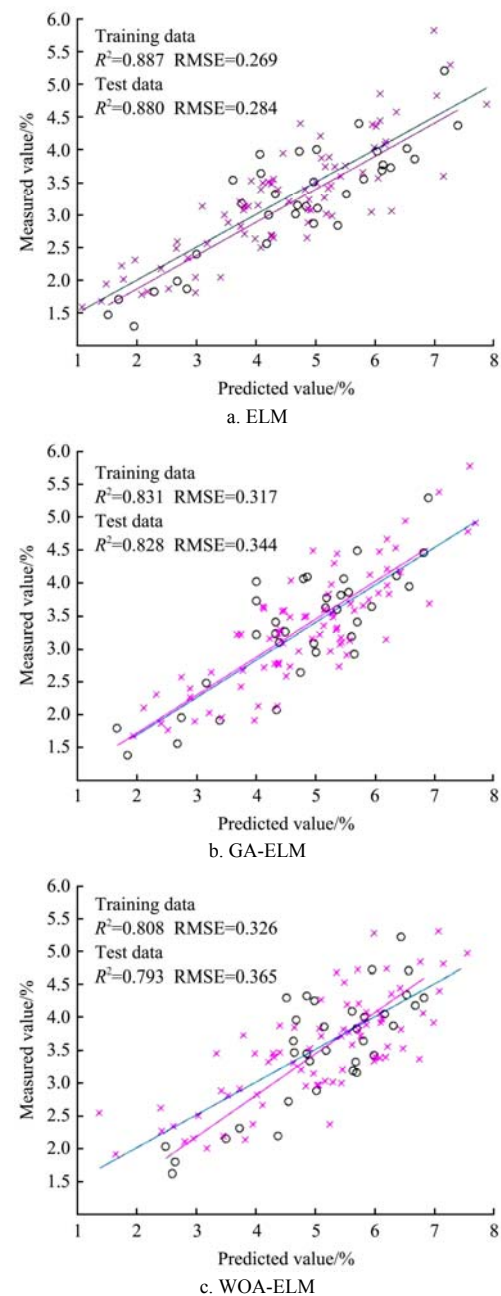
b. GA-ELM

c. WOA-ELM

Figure 5   Results of three modeling methods

It can be seen from the inversion results that the prediction effect of the limit learning machine optimized by WOA-ELM is obviously better than the inversion model established by simple ELM and GA-ELM.

This study attempts to extract the characteristic band of hyperspectral reflectance of rice canopy obtained by UAV through SPA method, optimize the weight and threshold of limit learning machine by whale algorithm, and finally establish the UAV remote sensing inversion model of rice nitrogen content, so as to realize the rapid monitoring and evaluation of UAV remote sensing diagnosis of rice canopy leaf nitrogen content in cold area. The traditional single or multiple regression statistical model based on hyperspectral characteristic band may not be able to fully express the nonlinear mathematical relationship between hyperspectral Information and nitrogen content, and to some extent, it restricts the accuracy of nitrogen content inversion. Therefore, in this study, WOA-ELM was used as the input of rice hyperspectral characteristic band to establish the nitrogen content inversion model.

The accuracy of WOA-ELM model is better than that of elm and GA-ELM. This is because the WOA algorithm optimizes the input weight of the limit learning machine and the threshold value of the hidden layer, and avoids the disadvantages of poor generalization ability and low calibration accuracy caused by randomly given input weight and the threshold value of the hidden layer when the number of hidden layer nodes is small. The characteristic band selected in this study is basically the same as the previous conclusion in the range of characteristic band, but the specific characteristic band is not the same. The main reasons are as follows: 1) there is a certain degree of difference in characteristic bands due to different varieties. 2) due to the interference of surface features such as water, weeds and soil in rice field, the above-mentioned spectral information may be mixed in the process of rice pure Hyperspectral Information Extraction, which may also result in different feature band extraction.

In this study, the UAV hyperspectral remote sensing platform is used, which has some acquisition errors. Therefore, in the future research, we will increase the experimental varieties, and establish the inversion model of chlorophyll content for different growth stages of rice, to improve the accuracy and of the model.

4   Conclusions

In this paper, based on the hyperspectral remote sensing data of rice canopy UAV, combined with the nitrogen content of rice on the ground, the characteristic bands which can represent the hyperspectral Information of rice canopy were extracted by continuous projection method. On this basis, the inversion model of nitrogen content in rice canopy was established by using the optimized elm algorithm of WOA. The conclusions are as follows:

(1) The hyperspectral characteristic bands which can represent the range of 400~1000 nm are extracted by SPA algorithm. The characteristic bands selected in this study are 465 nm, 501 nm, 578 nm, 702 nm and 783 nm, respectively.

(2) In the model adopted in this study, WOA-ELM has the highest accuracy, the R^2 of training data is 0.887, the R^2 of test data is 0.880, the RMSE of training data is 0.269, the RMSE of test data is 0.284. The model shows a good prediction ability, which can provide a certain data support and model reference for the inversion research and nutrient diagnosis of rice nitrogen content in cold region.

Acknowledgments

[References]

[1] Tan K Z, Wang S W, Song Y Z, Liu Y, Gong Z P. Estimating nitrogen status of rice canopy using hyperspectral reflectance combined with BPSO-SVR in cold region. Chemometrics Intell Lab Syst, 2018; 172: 68–79.   doi: 10.1016/j.chemolab.2017.11.014

[2] Li X P, Ma W D, Chang W, Liang C, Zhao H X, Guo JX, et al. Linkage Disequilibrium Analysis of Rice Sheath Blight Resistance Markers of Rice Grown in the Cold Region of Northeast China. Genetika-Belgrade, 2018; 50(3): 943–58. doi: 10.2298/Gensr1803943l

[3] Kawamura K, Ikeura H, Phongchanmaixay S, Khanthavong P. Canopy Hyperspectral Sensing of Paddy Fields at the Booting Stage and PLS Regression can Assess Grain Yield. Remote Sens, 2018; 10(8): 15. doi: 10.3390/rs10081249

[4] Dayananda S, Astor T, Wijesingha J, Thimappa SC, Chowdappa H D, Mudalagiriyappa, et al. Multi-Temporal Monsoon Crop Biomass Estimation Using Hyperspectral Imaging. Remote Sens, 2019; 11(15): 19. doi: 10.3390/rs11151771

[5] Nutini F, Confalonieri R, Crema A, Movedi E, Paleari L, Stavrakoudis D, et al. An operational workflow to assess rice nutritional status based on satellite imagery and smartphone apps. Comput Electron Agric, 2018; 154: 80–92. doi: 10.1016/j.compag.2018.08.008

[6] Zheng H B, Cheng T, Li D, Yao X, Tian Y C, Cao W X, et al. Combining Unmanned Aerial Vehicle (UAV)-Based Multispectral Imagery and Ground-Based Hyperspectral Data for Plant Nitrogen Concentration Estimation in Rice. Front Plant Sci 2018; 9: 13. doi: 10.3389/fpls.2018.00936

[7] Yu F H, Xu T Y, Cao Y L, Yang G J, Du W, Wang S. Models for estimating the leaf NDVI of japonica rice on a canopy scale by combining canopy NDVI and multisource environmental data in Northeast China. Int J Agric Biol Eng, 2016; 9(5): 132–42. doi: 10.3965/ j.ijabe.20160905.2266

[8] Li S Y, Ding X Z, Kuang Q L, Ata-Ul-Karim S T, Cheng T, Liu X J, et al. Potential of UAV-Based Active Sensing for Monitoring Rice Leaf Nitrogen Status. Front Plant Sci, 2018; 9: 14. doi: 10.3389/fpls.2018.01834

[9] Yu F H, Xu T Y, Du W, Ma H, Zhang G S, Chen C L. Radiative transfer models (RTMs) for field phenotyping inversion of rice based on UAV hyperspectral remote sensing. Int J Agric Biol Eng, 2017; 10(4): 150–7. doi: 10.25165/j.ijabe.20171004.3076

[10] Du W, Xu T Y, Yu F H, Chen C L. Measurement of nitrogen content in rice by inversion of hyperspectral reflectance data from an unmanned aerial vehicle. Cienc Rural, 2018; 48(6): 10. doi: 10.1590/ 0103-8478cr20180008

[11] Jay S, Baret F, Dutartre D, Malatesta G, Heno S, Comar A, et al. Exploiting the centimeter resolution of UAV multispectral imagery to improve remote-sensing estimates of canopy structure and biochemistry in sugar beet crops. Remote Sens Environ, 2019; 231: 17. doi: 10.1016/j.rse.2018.09.011

[12] Camino C, González-Dugo V, Hernández P, Sillero J C, Zarco‐Tejada PJ. Improved nitrogen retrievals with airborne-derived fluorescence and plant traits quantified from VNIR-SWIR hyperspectral imagery in the context of precision agriculture. International Journal of Applied Earth Observation and Geoinformation, 2018; 70: 105–17. doi: 10.1016/j.jag.2018.04.013

[13] Klem K, Zahora J, Zemek F, Trunda P, Tuma I, Novotna K, et al. Interactive effects of water deficit and nitrogen nutrition on winter wheat. Remote sensing methods for their detection. Agric Water Manage, 2018; 210: 171–84. doi: 10.1016/j.agwat.2018.08.004

[14] Lussem U, Bolten A, Menne J, Gnyp M L, Schellberg J, Bareth G. Estimating biomass in temperate grassland with high resolution canopy surface models from UAV-based RGB images and vegetation indices. J Appl Remote Sens, 2019; 13(3): 26. doi: 10.1117/1.Jrs.13.034525

[15] Hashimoto N, Saito Y, Maki M, Homma K. Simulation of Reflectance and Vegetation Indices for Unmanned Aerial Vehicle (UAV) Monitoring of Paddy Fields. Remote Sens, 2019; 11(18): 13. doi: 10.3390/rs11182119

[16] Duan B, Liu Y T , Gong Y, Peng Y, Wu X T, Zhu R S, et al. Remote estimation of rice LAI based on Fourier spectrum texture from UAV image. Plant Methods, 2019; 15(1): 12. doi: 10.1186/s13007-019-0507-8

[17] Shen X, Cao L, Yang B S, Xu Z, Wang G B. Estimation of Forest Structural Attributes Using Spectral Indices and Point Clouds from

UAS-Based Multispectral and RGB Imageries.   Remote Sens, 2019; 11(7): 24.   doi: 10.3390/rs11070800

[18] Abdulridha J, Batuman O, Ampatzidis Y.   UAV-Based Remote Sensing Technique to Detect Citrus Canker Disease Utilizing Hyperspectral Imaging and Machine Learning.   Remote Sens, 2019; 11(11): 22.   doi: 10.3390/rs11111373

[19] Ge X Y, Wang J Z, Ding J L, Cao X Y, Zhang Z P, Liu J, et al.   Combining UAV-based hyperspectral imagery and machine learning algorithms for soil moisture content monitoring.   PeerJ, 2019; 7: 27.   doi: 10.7717/ peerj.6926

[20] Madlikova M, Krausova I, Mizera J, Taborsky J, Famera O, Chvatil D. Nitrogen assay in winter wheat by short-time instrumental photon activation analysis and its comparison with the Kjeldahl method.   J Radioanal Nucl Chem, 2018; 317(1): 479–86.   doi: 10.1007/ s10967-018-5881-6